Optical Half-Band Filters

Kaname Jinguji and Manabu Oguma

***Abstract*—This paper proposes two kinds of novel 2 × 2 circuit configuration for finite-impulse response (FIR) half-band filters. These configurations can be transformed into each other by a symmetric transformation and their power transmittance is identical. The configurations have only about half the elements of conventional FIR lattice-form filters. We derive a design algorithm for achieving desired power transmittance spectra. We also describe 2 × 2 circuit configurations for infinite-impulse response (IIR) half-band filters. These configurations are designed to realize arbitrary-order IIR half-band filter characteristics by extending the conventional half-band circuit configuration used in millimeter-wave devices. We discuss their filter characteristics and confirm that they have a power half-band property. We demonstrate design examples including FIR maximally flat half-band filters, an FIR Chebyshev half-band filter, and an IIR elliptic half-band filter.**

***Index Terms*—Chebyshev, design, elliptic, finite-impulse response (FIR), half-band, infinite-impulse response (IIR), Mach–Zehnder, maximally flat, optical, synthesis, waveguide.**

I. Introduction

OPTICAL delay-line circuits [1]–[3] are widely used in the field of optical signal processing. They are composed of optical waveguides operating as optical delay lines, directional couplers, and phase shifters. A wide variety of functions can be realized with these circuits by adjusting their directional couplers and phase shifters since their transmission characteristics are the same as those of electric digital filters. Several useful devices have been reported including add/drop multiplexing filters [4]–[6], an EDFA gain equalization filter [7], a polarization mode dispersion equalizer [8], and a variable group-delay dispersion equalizer [9]–[11]. Since most of these devices have 2 × 2 circuit configurations, this paper focuses on 2 × 2 optical half-band filters.

Optical delay-line circuits are roughly classified into finite-impulse response (FIR) filters and infinite-impulse response (IIR) filters [12]. FIR filters consist simply of feedforward waveguides, and their impulse responses are limited in finite time. IIR filters include feedback loops such as ring waveguides, and their impulse responses continue for infinite time. A typical 2 × 2 circuit configuration of FIR optical filters is the lattice form which is composed of cascaded 2 × 2 Mach–Zehnder interferometers (MZI's) with a unit path length difference of ΔL [13]. We have already developed a synthesis algorithm based on scattering matrix factorization for realizing arbitrary FIR filters including linear-phase Chebyshev filters [13]. We have also proposed a basic 2 × 2 circuit configuration and a synthesis algorithm for realizing arbitrary IIR filters [14]. The circuit configuration consists of some cascaded unit elements composed of a 2 × 2 MZI with a path length difference of zero and a ring waveguide with a unit path length of ΔL.

Recently, Madsen [15] proposed some novel and simpler 2 × 2 circuit configurations optimized for specific IIR optical filters such as elliptic filters. They are composed of an MZI with several ring waveguides. The path length difference of the MZI is zero. *Her* circuit configurations can be achieved by removing some directional couplers from our basic IIR circuit configuration. They correspond to robust structures with two allpass circuits [16] which are well known in the field of digital filters [17].

Optical half-band filters are important components of wavelength division multiplexing (WDM) systems. A 2 × 2 IIR circuit configuration with one or two feedback loops optimized for IIR half-band filters is already known, and this configuration has been used to realize a millimeter-wave waveguide circuit [18] and a millimeter-wave bulk filter with resonators [19]. An optical multi/demultiplexer with this configuration has also been fabricated [20] using silica-based planar lightwave circuits (PLC's) [21]. However, no optimized 2 × 2 circuit configurations have yet been reported for FIR optical half-band filters.

This paper proposes two kinds of novel 2 × 2 circuit configuration for FIR optical half-band filters. They can be transformed into each other by a symmetric transformation which reverses their input and output ports. We confirm that these FIR circuit configurations have a power half-band property. We also discuss generalized 2 × 2 IIR circuit configurations with $M + N$ ring waveguides for IIR optical half-band filters. We obtained these circuit configurations by extending the conventional IIR half-band circuit configuration with one or two ring waveguides to realize arbitrary-order half-band filter characteristics. This paper provides methods for designing FIR and IIR half-band filters, and describes design examples including FIR maximally flat half-band filters, an FIR Chebyshev half-band filter, and an IIR elliptic half-band filter.

II. Circuit Configuratios and Half-Band Filter Characteristics

A. Half-Band Filter Characteristics

Fig. 1 shows the power transmittance spectrum of a half-band filter. This spectrum has a power half-band property defined as

$$|G(\omega)|^2 + \left|G\left(\omega + \frac{\omega_0}{2}\right)\right|^2 = 1 \tag{1}$$

where

$G(\omega)$ transfer function;

ω_0 angular frequency period.

Manuscript received June 1, 1999; revised September 22, 1999.

The authors are with NTT Photonics Laboratories, Ibaraki-ken 319-1193, Japan (e-mail: jinguji@iba.iecl.ntt.co.jp).

Publisher Item Identifier S 0733-8724(00)01468-7.

Symmetric half-band filters are especially significant for practical applications, since their passband and stopband widths are the same. This symmetry can be described as

$$|G(\omega)|^2 = |G(-\omega)|^2. \tag{2}$$

Many useful filters such as maximally flat, Chebyshev, and elliptic half-band filters have this symmetric property. Although the term "half-band filter" is frequently used to mean symmetric half-band filters with the symmetry described by (2) and also used to mean amplitude half-band filters with the following property $G(\omega)+G(\omega+(\omega_0/2)) = 1$ [17], this paper deals with generalized power half-band filters defined only by the power half-band property (1) and includes asymmetric filters.

The power half-band property described as (1) can be rewritten as

$$G(z)G_*(z) + G(-z)G_*(-z) = 1. \tag{3}$$

The variable z indicates $e^{j\omega\Delta\tau}$, where unit delay time $\Delta\tau$ corresponding to unit path length ΔL is defined as $2\pi/\omega_0$ and angular frequency ω is extended to a complex number.

The subscript $*$ indicates a para-Hermitian conjugation defined as

$$G_*(z) = G^*\left(\frac{1}{z^*}\right). \tag{4}$$

This analysis based on the z variable is widely used in the field of digital filters [12], [17]. This paper deals solely with 2×2 optical half-band filters, and assumes that the optical waveguides are lossless. Their transfer functions have the following lossless property

$$G(z)G_*(z) + H(z)H_*(z) = 1 \tag{5}$$

where $G(z)$ and $H(z)$ are their bar and cross transfer functions. Therefore, the power half-band property (3) is also described as

$$G(z)G_*(z) = H(-z)H_*(-z) \tag{6}$$

for 2×2 lossless half-band filters. Here, the relation (6) is adopted as a definition of the power half-band property of 2×2 optical half-band filters.

B. FIR Half-Band Filters

Fig. 2(a) and (b) shows two kinds of novel 2×2 circuit configurations which we propose for FIR optical half-band filters. They are composed of $N-1$ MZI's with a path length difference of $2\Delta L$ and one MZI with a path length difference of ΔL. The MZI with a path length difference of ΔL is on the output-port side in Fig. 2(a), while it is on the input-port side in Fig. 2(b). The directional coupler near the output ports provides 3 dB-coupling in Fig. 2(a), while the directional coupler near input ports provides 3 dB-coupling in Fig. 2(b). Optical phase shifters are formed on the MZI's to control the phase difference of the two arms of each MZI.

The circuit configurations shown in Fig. 2(a) and (b) can be transformed into each other by a symmetric transformation which reverses their input and output ports. Since the maximum path difference between input and output ports is $(2N-1)\Delta L$

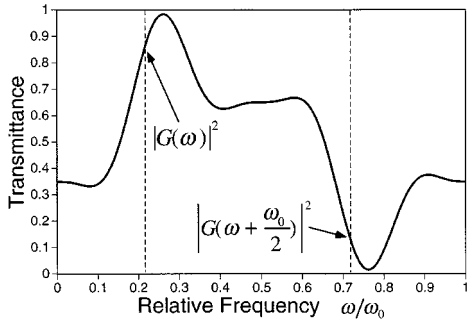

Fig. 1. Power half-band property defined as $|G(\omega)|^2+|G[\omega+(\omega_0/2)]|^2 = 1$, where ω_0 is the frequency period.

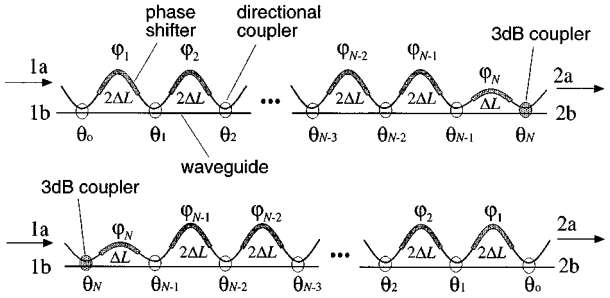

Fig. 2. Two kinds of 2×2 circuit configuration for FIR half-band filters are shown in (a) and (b). They are transformed into each other with a symmetric transformation which reverses their input and output ports, and have identical power transmittance characteristics.

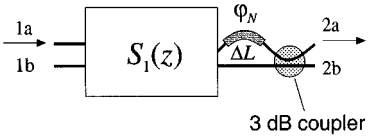

Fig. 3. Schematic circuit configuration of Fig. 2(a). S_1 indicates the transfer matrix of $N-1$ MZI's with a path length difference of $2\Delta L$.

in Fig. 2(a), the filter order is $2N-1$ and its transfer matrix can be written as

$$S(z) = \begin{pmatrix} G(z) & jH_*(z)z^{-(2N-1)} \\ jH(z) & G_*(z)z^{-(2N-1)} \end{pmatrix} \tag{7}$$

where $G(z)$ and $H(z)$ are its bar and cross $(2N-1)$th-order transfer functions, respectively. It is known that the transfer matrices of reciprocal devices are transposed by the symmetric transformation which reverses their input and output ports [22]. Therefore, the transfer matrix of the transformed circuit configuration shown in Fig. 2(b) can be written as

$$\tilde{S}(z) = \begin{pmatrix} G(z) & jH(z) \\ jH_*(z)z^{-(2N-1)} & G_*(z)z^{-(2N-1)} \end{pmatrix}. \tag{8}$$

This result indicates that the two circuit configurations in Fig. 2(a) and (b) have the same power transmittance spectra. Consequently, it is only necessary to consider the circuit configuration in Fig. 2(a) when designing FIR half-band filters.

Fig. 3 is a diagram of the circuit configuration in Fig. 2(a). Let the transfer matrix of the $N-1$ MZI's with a path length difference of $2\Delta L$ be

$$S_1(z) = \begin{pmatrix} G_1(z) & jH_{1^*}(z)z^{-2(N-1)} \\ jH_1(z) & G_{1^*}(z)z^{-2(N-1)} \end{pmatrix} \tag{9}$$

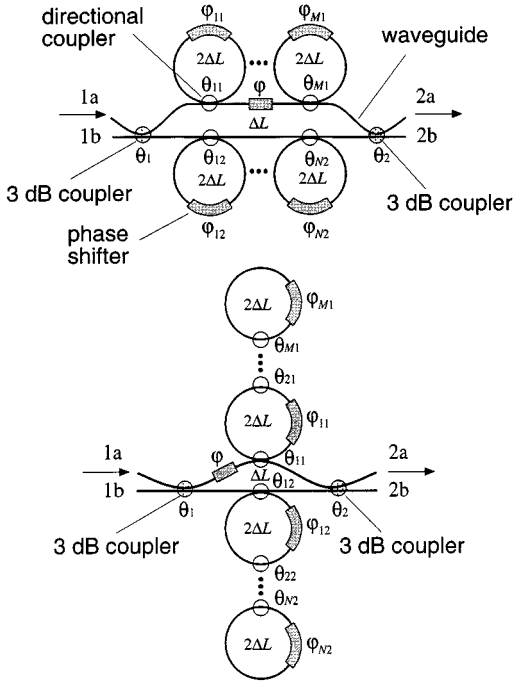

Fig. 4. Two kinds of extended 2 × 2 circuit configuration for IIR half-band filters are shown in (a) and (b).

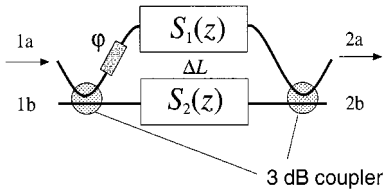

Fig. 5. Schematic circuit configuration of Fig. 4(a) and (b).

where $G_1(z)$ and $H_1(z)$ are its bar and cross transfer functions. In the above equation, $G_1(z)$ and $H_1(z)$ are given as

$$G_1(z) = \sum_{k=0}^{N-1} a_{2k,1} z^{-2k} \tag{10}$$

$$H_1(z) = \sum_{k=0}^{N-1} b_{2k,1} z^{-2k} \tag{11}$$

since each path length difference of the $N-1$ MZI's is $2\Delta L$. The bar and cross transfer functions $G(z)$ and $H(z)$ of the total circuit can be obtained with $G_1(z)$ and $H_1(z)$ as

$$G(z) = \frac{1}{\sqrt{2}}(G_1(z)z^{-1}e^{-j\varphi_N} + H_1(z)) \tag{12}$$

$$H(z) = \frac{1}{\sqrt{2}}(-G_1(z)z^{-1}e^{-j\varphi_N} + H_1(z)). \tag{13}$$

From (12) and (13), $H(-z)$ can be calculated as follows:

$$\begin{aligned} H(-z) &= \frac{1}{\sqrt{2}}(-G_1(-z)(-z)^{-1}e^{-j\varphi_N} + H_1(-z)) \\ &= \frac{1}{\sqrt{2}}(G_1(z)z^{-1}e^{-j\varphi_N} + H_1(z)) = G(z). \end{aligned} \tag{14}$$

TABLE I
POWER EXPANSION COEFFICIENTS, AMPLITUDE EXPANSION COEFFICIENTS, AND CIRCUIT PARAMETERS FOR FIR MAXIMALLY-FLAT HALF-BAND FILTERS ($N = 2, 3$, AND 4)

	k	bar power expansion coefficients A_k	bar expansion coefficients a_k	cross expansion coefficients b_k	circuit parameters (xπ)	
N=2	0	0.5	0.09151	0.09151	θ_0	0.0833
	1	0.28125	-0.15850	0.15850	θ_1	0.3333
	2	0.0	-0.59151	-0.59151	θ_2	0.25
	3	-0.03125	-0.34150	0.34150	φ_1	1.0
					φ_2	0.0
	k	bar power expansion coefficients A_k	bar expansion coefficients a_k	cross expansion coefficients b_k	circuit parameters (xπ)	
N=3	0	0.5	0.23526	0.23526	θ_0	0.4664
	1	-0.29297	0.57057	-0.57057	θ_1	0.1591
	2	0.0	0.32514	0.32514	θ_2	0.3755
	3	0.04883	-0.09548	0.09548	θ_3	0.25
	4	0.0	-0.06040	0.06040	φ_1	0.0
	5	-0.00586	0.02491	-0.02491	φ_2	1.0
					φ_3	0.0
	k	bar power expansion coefficients A_k	bar expansion coefficients a_k	cross expansion coefficients b_k	circuit parameters (xπ)	
N=4	0	0.5	0.05358	0.05358	θ_0	0.3720
	1	-0.29907	0.02095	-0.02095	θ_1	0.2860
	2	0.0	-0.35188	-0.35188	θ_2	0.4547
	3	0.05981	-0.56833	0.56833	θ_3	0.1187
	4	0.0	-0.21061	-0.21061	θ_4	0.25
	5	-0.01196	0.07016	-0.07016	φ_1	1.0
	6	0.0	0.00891	0.00891	φ_2	0.0
	7	0.00122	-0.02278	0.02278	φ_3	1.0
					φ_4	0.0

In the above equation, we use the relations $G_1(-z) = G_1(z)$, $H_1(-z) = H_1(z)$, which can be derived from (10), (11). It is confirmed from (14) that the circuit configurations satisfy the power half-band requirement defined by (6).

It can be understood from (12), (13) that a circuit configuration with N MZI's realizes $(2N-1)$th-order filter characteristics. This means our circuit configurations require about half the optical elements of conventional FIR lattice-form filters which realizes $(2N-1)$th-order filter characteristics with $2N-1$ MZI's. It should be noted that our circuit configurations can realize only odd-order half-band characteristics. The half-band circuit condition defined as (14) is necessary for realizing FIR half-band filters with our circuit configurations. This is mentioned in detail in Section III-A.

C. IIR Half-Band Filters

Fig. 4(a) and (b) shows 2 × 2 circuit configurations for IIR half-band filters. The circuit configurations consist of an MZI whose two arms are connected with a number of ring waveg-

uides with a path length of $2\Delta L$. The path length difference between the two arms is ΔL. The two directional couplers on each side of the MZI provide 3 dB-coupling. The conventional 2 $\times$ 2 half-band circuit configuration used in the millimeter-wave system field corresponds to the case incorporating one or two ring waveguides [18], [19]. Here, the conventional configuration is extended to circuit configurations with M upper rings and N lower rings to realize arbitrary-order IIR filter characteristics. Though the ring waveguides are connected in a different way in Fig. 3(a) and (b), the circuit configurations can realize identical transmission characteristics by providing each circuit configuration with appropriate circuit parameters. These circuit configurations correspond to special cases of Madsen's circuits [15], whose transmission characteristics have already been discussed [15], [16].

Fig. 5 shows the schematic circuit configuration of Fig. 4(a) and (b). The transfer functions $S_1(z)$ and $S_2(z)$ are allpass functions which consist of multiring waveguides in Fig. 4(a) and (b). The bar and cross transfer functions $G(z)$ and $H(z)$ of the total circuit are calculated as

$$G(z) = \tfrac{1}{2}(S_1(z)z^{-1}e^{-j\varphi} - S_2(z)) \tag{15}$$

$$H(z) = -\tfrac{1}{2}(S_1(z)z^{-1}e^{-j\varphi} + S_2(z)). \tag{16}$$

The allpass functions $S_1(z)$ and $S_2(z)$ are generally described as

$$S_1(z) = \frac{e^{-j\Psi_1}z^{-2M}D_{1^*}(z)}{D_1(z)} \tag{17}$$

$$S_2(z) = \frac{e^{-j\Psi_2}z^{-2N}D_{2^*}(z)}{D_2(z)} \tag{18}$$

where the z polynomials $D_1(z)$ and $D_2(z)$ are written as

$$D_1(z) = 1 + \sum_{k=1}^{M} d_{2k,1}z^{-2k} \tag{19}$$

$$D_2(z) = 1 + \sum_{k=1}^{N} d_{2k,2}z^{-2k} \tag{20}$$

since the path length of each ring waveguide is $2\Delta L$. In (17) and (18), it is assumed that Ψ_1 and Ψ_2 have the relation $\Psi_1 + \Psi_2 + \varphi = 0$. This relation has no influence on the transmission characteristics. It can be understood from (15) and (16) that a circuit configuration with M upper rings and N lower rings realizes $(2M+2N+1)$th-order filter characteristics. For example, when $M = 1$ and $N = 2$, seventh-order filter characteristics are realized. Thus, only odd-order IIR half-band characteristics are realized with our circuit configurations. The following relationship between $G(z)$ and $H(z)$ can be obtained from (15) and (16)

$$\begin{aligned} H(-z) &= -\tfrac{1}{2}(S_1(-z)(-z)^{-1}e^{-j\varphi} + S_2(-z)) \\ &= \tfrac{1}{2}(S_1(z)z^{-1}e^{-j\varphi} - S_2(z)) = G(z). \end{aligned} \tag{21}$$

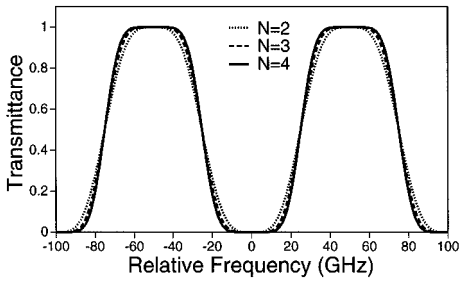

Fig. 6. Bar power transmittance spectra of FIR maximally flat half-band filters ($N = 2, 3$, and 4).

TABLE II
POWER EXPANSION COEFFICIENTS, AMPLITUDE EXPANSION COEFFICIENTS, AND CIRCUIT PARAMETERS FOR FIR CHEBYSHEV HALF-BAND FILTER ($N = 4$)

k	bar power expansion coefficients A_k	bar expansion coefficients a_k	cross expansion coefficients b_k	circuit parameters (xπ)	
0	0.5	0.11091	0.11091	θ_0	0.3498
1	0.30717	0.02835	-0.02835	θ_1	0.2448
2	0.0	-0.35699	-0.35699	θ_2	0.4186
3	-0.07797	-0.54316	0.54316	θ_3	0.0797
4	0.0	-0.24255	-0.24255	θ_4	0.25
5	0.02581	0.04683	-0.04683	φ_1	1.0
6	0.0	0.01447	0.01447	φ_2	0.0
7	-0.00628	-0.05659	0.05659	φ_3	1.0
				φ_4	0.0

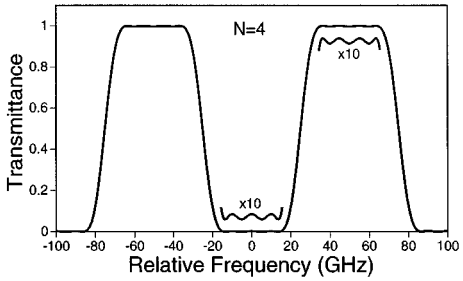

Fig. 7. Bar power transmittance spectrum of FIR Chebyshev half-band filter ($N = 4$).

In the above equation, we use the relations $S_1(-z) = S_1(z)$, $S_2(-z) = S_2(z)$, which are derived from (17)–(20). It is confirmed from (21) that the transfer functions $G(z)$ and $H(z)$ satisfy the power half-band requirement (6).

Since the circuit configurations of Fig. 4(a) and (b) correspond to the special cases of Madsen's circuit configurations [15], the numerator polynomials $P(z)$ and $Q(z)$ of $G(z)$ and $H(z)$ must have the same symmetry as Madsen's. The symmetry relations are expressed as

$$P(z) = -P_*(z)z^{-(2M+2N+1)} \tag{22}$$

$$Q(z) = Q_*(z)z^{-(2M+2N+1)}. \tag{23}$$

These relations indicate that when $P(z)$ and $Q(z)$ have real coefficients, $P(z)$ is antisymmetric and $Q(z)$ is symmetric. These conditions are necessary for synthesizing Madsen's circuit configurations. Therefore, we require both the half-band circuit condition (21) and the symmetry conditions (22), (23) to realize IIR half-band filters with the circuit configurations of Fig. 4(a) and (b).

III. Design Algorithm and Design Examples of FIR Half-Band Filters

A. Algorithm for Designing FIR Half-Band Filters

Power transmission characteristics of FIR half-band filters can be written as

$$G(z)G_*(z) = \tfrac{1}{2} + \left(\sum_{k=1}^{N} A_{2k-1} z^{-(2k-1)} + \sum_{k=1}^{N} A_{-(2k-1)} z^{2k-1}\right) \quad (24)$$

$$H(z)H_*(z) = \tfrac{1}{2} - \left(\sum_{k=1}^{N} A_{2k-1} z^{-(2k-1)} + \sum_{k=1}^{N} A_{-(2k-1)} z^{2k-1}\right) \quad (25)$$

where A_{2k-1} has the relation $A_{2k-1} = A^*_{-(2k-1)}$, since $(G(z)G_*(z))_* = G(z)G_*(z)$. Here, it is assumed that the power expansion coefficients A_{2k-1} $(K = 1, \ldots, N)$ are given for a desired power transmittance spectrum. It can be confirmed in (24) and (25) that $G(z)G_*(z)$ and $H(z)H_*(z)$ satisfy both the lossless requirement (5) and the power half-band requirement (6).

Our design algorithm consists of two parts. The purpose of the first procedure is to find bar and cross amplitude expansion coefficients a_k and b_k that satisfy the half-band circuit condition $G(z) = H(-z)$ described in Section II-B, from the given power expansion coefficients. The purpose of the second procedure is to calculate the circuit parameters θ_k and φ_k shown in Fig. 2(a) and (b) from the obtained amplitude expansion coefficients a_k and b_k.

The steps in the first procedure are summarized as follows.

1) Calculate the zeros of $G(z)G_*(z)$ and $H(z)H_*(z)$. The power half-band property (6) means that when $G(z)G_*(z)$ has a set of zero pairs $\{(\alpha_1, 1/\alpha_1^*), (\alpha_2, 1/\alpha_2^*), \cdots, (\alpha_{2N-1}, 1/\alpha_{2N-1}^*)\}$, $H(z)$ $H_*(z)$ has a corresponding set of zero pairs $\{(-\alpha_1, -1/\alpha_1^*), (-\alpha_2, -1/\alpha_2^*), \cdots, (-\alpha_{2N-1}, -1/\alpha_{2N-1}^*)\}$.
2) Obtain a zero set $\{\alpha_k\}$ of $G(z)$ and a zero set $\{-\alpha_k\}$ of $H(z)$ by choosing one zero from each zero pair $(\alpha_k, 1/\alpha_k^*)$ of $G(z)G_*(z)$ and one zero from each zero pair $(-\alpha_k, -1/\alpha_k^*)$ of $H(z)H_*(z)$, respectively. They have to be carefully chosen, so that they satisfy the half-band circuit condition $G(z) = H(-z)$, that is, when α_k of a zero pair $(\alpha_k, 1/\alpha_k^*)$ is chosen for $G(z)$, $-\alpha_k$ of the corresponding zero pair $(-\alpha_k, -1/\alpha_k^*)$ has to be chosen for $H(z)$. For example, consider $G(z)G_*(z)$ with a set of zero pairs $\{(\alpha_1, 1/\alpha_1^*), (\alpha_2, 1/\alpha_2^*), (\alpha_3, 1/\alpha_3^*)\}$ and $H(z)H_*(z)$ with a corresponding set of zero pairs $\{(-\alpha_1, -1/\alpha_1^*), (-\alpha_2, -1/\alpha_2^*), (-\alpha_3, -1/\alpha_3^*)\}$. When zeros $\{\alpha_1, 1/\alpha_2^*, 1/\alpha_3^*\}$ are chosen for $G(z)$, the corresponding zeros $\{-\alpha_1, -1/\alpha_2^*, -1/\alpha_3^*\}$ have to be chosen for $H(z)$.
3) Calculate $G(z)$ and $H(z)$ as

$$G(z) = a_0 \prod_{k=1}^{2N-1} (1 - \alpha_k z^{-1}) \quad (26)$$

$$H(z) = a_0 \prod_{k=1}^{2N-1} (1 + \alpha_k z^{-1}) \quad (27)$$

where a_0 is given by

$$a_0 = \sqrt{\frac{1}{\prod_{k=1}^{2N-1} (1-\alpha_k)(1-\alpha_k^*) + \prod_{k=1}^{2N-1} (1+\alpha_k)(1+\alpha_k^*)}} \quad (28)$$

so that the lossless property (5) may be satisfied.

Thus, when $G(z)G_*(z)$ and $H(z)H_*(z)$ that satisfy the power half-band requirement (6) are given, $G(z)$ and $H(z)$ that satisfy the half-band circuit condition $G(z) = H(-z)$ are always found by using the above steps.

The second procedure is based on the synthesis algorithm for FIR lattice-form filters [13]. From (12) and (13), the transfer functions $G_1(z)$ and $H_1(z)$ of S_1 in Fig. 3 can be obtained as

$$G_1(z) = \frac{1}{\sqrt{2}}(G(z) - H(z))z \quad (29)$$

$$H_1(z) = \frac{1}{\sqrt{2}}(G(z) + H(z)), \quad (30)$$

where φ_N is taken as 0. $G(z)$ and $H(z)$ that satisfy $G(z) = H(-z)$ can be written as

$$G(z) = \sum_{k=0}^{N-1} a_{2k} z^{-2k} + \sum_{k=0}^{N-1} a_{2k+1} z^{-(2k+1)} \quad (31)$$

$$H(z) = \sum_{k=0}^{N-1} a_{2k} z^{-2k} - \sum_{k=0}^{N-1} a_{2k+1} z^{-(2k+1)}. \quad (32)$$

By substituting these $G(z)$ and $H(z)$ in (29) and (30), $G_1(z)$ and $H_1(z)$ can be obtained as

$$G_1(z) = \sqrt{2} \sum_{k=0}^{N-1} a_{2k+1} z^{-2k} \quad (33)$$

$$H_2(z) = \sqrt{2} \sum_{k=0}^{N-1} a_{2k} z^{-2k}. \quad (34)$$

It is confirmed from the above equations that $G_1(z)$ and $H_1(z)$ are polynomials of z^{-2}. Thus, the condition $G(z) = H(-z)$ is necessary for guaranteeing that $G_1(z)$ and $H_1(z)$ are polynomials of z^{-2}. This means that the relation $G(z) = H(-z)$ is the condition necessary for realizing FIR half-band filters with our circuit configurations. The circuit parameters included in

$S_1(z)$ can be calculated by adopting the synthesis algorithm of FIR lattice-form filters for the obtained $G_1(z)$ and $H_1(z)$. This algorithm provides a unique set of circuit parameters for given bar and cross amplitude expansion coefficients a_k and b_k.

B. Design Examples of FIR Symmetric Half-Band Filters

1) Maximally Flat Half-Band Filters: The power transmission characteristics of FIR symmetric half-band filters can be written as

$$G(z)G_*(z) = \tfrac{1}{2} + \sum_{k=1}^{N} A_{2k-1}\left(z^{-(2k-1)} + z^{2k-1}\right) \quad (35)$$

$$H(z)H_*(z) = \tfrac{1}{2} - \sum_{k=1}^{N} A_{2k-1}\left(z^{-(2k-1)} + z^{2k-1}\right) \quad (36)$$

where A_{2k-1} is real, since $(G(z)G_*(z))_* = G(z)G_*(z)$. It can be confirmed that $G(z)G_*(z)$ and $H(z)H_*(z)$ have the lossless property (5), the power half-band property (6), and the symmetry (2) which is also rewritten as $G(z)G_*(z) = G(z^{-1})G_*(z^{-1})$. For maximally flat half-band filters, it is known that the power expansion coefficients are given by

$$A_{2k-1} = \frac{(-1)^{k+N}\prod_{i=1}^{2N}\left(N+\frac{1}{2}-i\right)}{2(N-k)!(N-1+k)!\left(\frac{1}{2}-k\right)} \quad (37)$$

where $k = 1, 2, \cdots, N$ [23].

The results for $N = 2, 3, 4$ are summarized in Table I. They correspond to third-order, fifth-order, and seventh-order maximally flat half-band filters, respectively. Here, θ_k is an angular representation of the coupling coefficient of the directional coupler, that is, $\sin\theta_k$ indicates the amplitude coupling ratio. For example, when $\theta_k = \pi/4$, the angle θ_k corresponds to 3 dB-coupling. Fig. 6 shows the bar power transmission spectra for $N = 2, 3, 4$. The frequency period is taken as 100 GHz. It can be confirmed that maximally flat half-band is realized in each power transmittance spectrum.

2) Chebyshev Half-Band Filter: Next, we provide a design example of a seventh-order FIR Chebyshev half-band filter. The corresponding $N = 4$. The power expansion coefficients were calculated by using the McClellan–Parks–Rabiner (MPR) algorithm [24]. The power expansion coefficients, the obtained amplitude expansion coefficients, and the circuit parameters are summarized in Table II. Fig. 7 shows the bar power transmittance spectrum of the seventh-order Chebyshev half-band filter calculated based on the circuit parameters. The frequency period is taken as 100 GHz. The ripple deviation of the power transmittance at the passbands and the stopbands is 2.54×10^{-3}.

IV. Design Algorithm and Design Examples of IIR Half-Band Filters

A. Algorithm for Designing IIR Half-Band Filters

Let the bar and cross transfer functions $G(z)$ and $H(z)$ of an IIR half-band filter be expressed as

$$G(z) = \frac{P(z)}{D(z)} = \frac{\sum_{k=0}^{2M+2N+1} p_k z^{-k}}{1 + \sum_{k=1}^{2M+2N+1} d_k z^{-k}} \quad (38)$$

$$H(z) = \frac{Q(z)}{D(z)} = \frac{\sum_{k=0}^{2M+2N+1} q_k z^{-k}}{1 + \sum_{k=1}^{2M+2N+1} d_k z^{-k}}. \quad (39)$$

As mentioned in Section II-C, $G(z)$ and $H(z)$ must satisfy both the half-band circuit condition (21) and the symmetry conditions of Madsen's circuits (22) and (23). The half-band circuit condition (21) can be rewritten as

$$P(z) = Q(-z) \quad (40)$$

$$D(z) = D(-z). \quad (41)$$

Here, it is assumed that $P(z)$, $Q(z)$, and $D(z)$ are given, and are described as

$$P(z) = \sum_{k=0}^{M+N} p_{2k} z^{-2k} + \sum_{k=0}^{M+N} p_{2k+1} z^{-(2k+1)} \quad (42)$$

$$Q(z) = \sum_{k=0}^{M+N} p_{2k} z^{-2k} - \sum_{k=0}^{M+N} p_{2k+1} z^{-(2k+1)} \quad (43)$$

$$D(z) = 1 + \sum_{k=1}^{M+N} d_{2k} z^{-2k} \quad (44)$$

where p_k and q_k satisfy

$$p_k = -p^*_{2M+2N+1-k} \quad (45)$$

$$q_k = q^*_{2M+2N+1-k} \quad (46)$$

which correspond to the symmetry conditions (22), (23).

For some IIR symmetric filters with real expansion coefficients including Chebyshev filters and elliptic filters, the algorithms for obtaining their amplitude expansion coefficients have already been developed [12], [17]. Since it is known through these algorithms that these filters satisfy the symmetry conditions of Madsen's circuits [15], [16], only the half-band circuit condition (21) has to be considered when designing IIR half-band filters. It is easy to obtain amplitude expansion coefficients that satisfy the half-band circuit condition by optimizing certain filter parameters. For instance, we calculated the amplitude expansion coefficients that satisfy the half-band circuit condition by optimizing both the passband edge frequency and

TABLE III
AMPLITUDE EXPANSION COEFFICIENTS AND CIRCUIT PARAMETERS FOR IIR ELLIPTIC HALF-BAND FILTER ($M = 1, N = 1$)

k	bar expansion coefficients p_k	cross expansion coefficients q_k	denominator expansion coefficients d_k	circuit parameters (xπ)	
0	0.08500	0.08500	1.0000	θ_1	0.25
1	-0.31631	0.31631	0.0	θ_2	0.25
2	0.55378	0.55378	0.80261	θ_{11}	0.2820
3	-0.55378	0.55378	0.0	θ_{12}	0.4456
4	0.31631	0.31631	0.10754	φ	0.0
5	-0.08500	0.08500	0.0	φ_{11}	1.0
				φ_{12}	1.0

the ripple deviation of the power transmittance in our example design of an elliptic filter described in Section IV-B.

From (15) and (16), the transfer functions $S_1(z)$ and $S_2(z)$ corresponding to the upper and lower allpass circuits in Fig. 5 can be obtained as

$$S_1(z) = (G(z) - H(z))z = \frac{(P(z) - Q(z))z}{D(z)} \tag{47}$$

$$S_2(z) = -(G(z) + H(z)) = \frac{P(z) + Q(z)}{D(z)} \tag{48}$$

where φ is taken as 0. $S_1(z)$ and $S_2(z)$ have to be all-pass functions, that is, $S_1(z)S_{1^*}(z) = 1$ and $S_2(z)S_{2^*}(z) = 1$. These are easily derived from the symmetry conditions of Madsen's circuits (22), (23) and the lossless condition (5). By substituting $P(z), Q(z)$ and $D(z)$ of (42)–(44) in the above equations, $S_1(z)$ and $S_2(z)$ can be obtained as

$$S_1(z) = \frac{2\sum_{k=0}^{M+N} p_{2k+1} z^{-2k}}{1 + \sum_{k=1}^{M+N} d_{2k} z^{-2k}} \tag{49}$$

$$S_2(z) = -\frac{2\sum_{k=0}^{M+N} p_{2k} z^{-2k}}{1 + \sum_{k=1}^{M+N} d_{2k} z^{-2k}}. \tag{50}$$

It can be seen that $S_1(z)$ and $S_2(z)$ are rational functions of z^{-2}. The half-band circuit condition (21) is necessary for guaranteeing that $S_1(z)$ and $S_2(z)$ are rational functions of z^{-2}. In the above equations, $S_1(z)$ and $S_2(z)$ have to be written as (17) and (18). This is guaranteed by the symmetry conditions of Madsen's circuits (22), (23), because the symmetry conditions guarantee that the circuit configuration shown in Fig. 5 is a Madsen's circuit. These facts mean that both the half-band circuit condition (21) and the symmetry conditions (22), (23) are necessary for realizing IIR half-band filters with the circuit configurations shown in Fig. 4(a) and (b). It is easy to calculate the circuit parameters included in allpass functions $S_1(z)$ and $S_2(z)$ by analyzing the poles of $S_1(z)$ and $S_2(z)$.

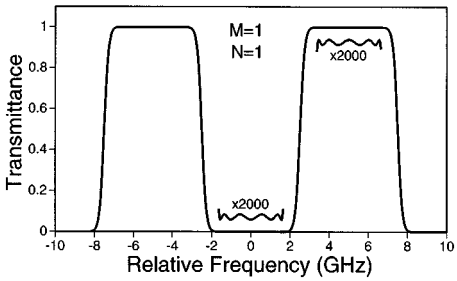

Fig. 8. Bar power transmittance spectrum of IIR elliptic half-band filter ($M = 1, N = 1$).

B. Design Example of IIR Elliptic Half-Band Filter

In this section, we describe a fifth-order IIR elliptic half-band filter. Its amplitude expansion coefficients are real. The corresponding M and N are 1 and 1, respectively. In this case, the circuit configurations of Fig. 4(a) and (b) are in agreement. Here, the necessary amplitude expansion coefficients were directly calculated by using the Gray–Markel (GM) algorithm [25] so that they may satisfy the half-band circuit condition $G(z) = H(-z)$.

The expansion coefficients and circuit parameters are summarized in Table III. Fig. 8 shows the bar power transmittance spectrum of the fifth-order elliptic half-band filter calculated based on the obtained circuit parameters. The frequency period is taken as 10 GHz. The ripple deviation of the power transmittance at the passbands and the stopbands is 1.27×10^{-5}.

V. CONCLUSION

This paper described two kinds of novel 2×2 circuit configuration for finite-impulse response (FIR) half-band filters. They consist of $N - 1$ MZI's with a path length difference of $2\Delta L$ and one MZI with a path length difference of ΔL. One configuration has the MZI with a path length difference of ΔL on the output-port side, while the other has it on the input-port side. The two circuit configurations can be transformed into each other with a symmetric transformation which reverses their input and output ports, and their power transmittance characteristics are identical. The FIR circuit configurations with N MZI's can realize $(2N - 1)$th-order FIR half-band filter characteristics. Therefore, they need only about half the elements of

conventional FIR lattice-form filters. We confirmed that our circuit configurations provide the required power half-band property. The condition necessary for realizing FIR half-band filters with our circuit configurations was obtained as $G(z) = H(-z)$, where $G(z)$ and $H(z)$ are bar and cross transfer functions, respectively. We derived an algorithm for determining the circuit parameters for our circuit configurations. We showed that we can always realize desired FIR half-band filters with our circuit configurations whether the filters are symmetric or not. We demonstrated a maximally flat half-band filters and a Chebyshev half-band filter as design examples of FIR half-band filters.

We also discussed 2×2 circuit configurations for infinite-impulse response (IIR) half-band filters. We obtained the circuit configurations by extending the conventional IIR half-band circuit configuration used in millimeter-wave devices to realize arbitrary-order half-band filter characteristics. They consist of one MZI with a path length difference of ΔL and two allpass circuits with a path length of $2\Delta L$ formed on each arm of the MZI. When the two all-pass circuits are composed of M rings and N rings, respectively, $(2M + 2N + 1)$th-order IIR half-band filter characteristics can be realized. We confirmed that these IIR circuit configurations have the required power half-band property. We showed that the half-band circuit condition $G(z) = H(-z)$ and the symmetry conditions of Madsen's circuits are necessary for realizing IIR half-band filters with the IIR half-band circuit configurations. We demonstrated an elliptic half-band filter as a design example of IIR half-band filters.

ACKNOWLEDGMENT

The authors would like to thank A. Himeno, Y. Ohmori, and Y. Hibino for their helpful suggestions and encouragement.

REFERENCES

[1] B. Moslehi, J. W. Goodman, M. Tur, and H. J. Shaw, "Fiber-optic lattice signal processing," *Proc. IEEE*, vol. 72, pp. 909–930, July 1984.
[2] K. P. Jackson, S. A. Newtons, B. Moslehi, M. C. C. Cuter, J. W. Goodman, and H. J. Shaw, "Optical fiber delay-line signal processing," *IEEE Trans. Microwave Theory Tech.*, vol. 33, pp. 193–208, Mar. 1985.
[3] K. P. Jackson, G. Xiao, and H. J. Shaw, "Coherent optical fiber delay line processor," *Electron. Lett.*, vol. 22, no. 25, pp. 1335–1337, 1986.
[4] C. Kostrzewa, R. Moosburger, G. Fischbeck, B. Schuppert, and K. Petermann, "Tunable polymer optical add/drop filter for multiwavelength networks," *IEEE Photon. Technol. Lett.*, vol. 9, pp. 1487–1489, Nov. 1997.
[5] B. J. Offrein, R. Germann, G. L. Bona, F. Horst, and H. W. M. Salemink, "Tunable optical add/drop components in silicon-oxynitride waveguide structures," in *Tech. Dig. ECOC'98*, 1998, pp. 325–326.
[6] R. Germann, R. Beyeler, G. L. Bona, F. Horst, B. J. Offrein, and H. W. M. Salemink, "Wavelength-tunable add/drop filter for optical networks," in *Tech. Dig. OFC'99*, vol. WM25-1, 1999.
[7] Y. P. Li, C. H. Henry, E. J. Laskowski, C. Y. Mak, and H. H. Yaffe, "A waveguide EDFA gain equalization filter," *Electron. Lett.*, vol. 31, no. 23, pp. 2005–2006, 1995.
[8] T. Ozeki and T. Kudo, "Adaptive equalization of polarization mode dispersion," in *Tech. Dig. OFC/IOOC'93*, 1993, paper FC-7.
[9] K. Jinguji, K. Takiguchi, and M. Kawachi, "Design of variable group-delay dispersion equalizer using a lattice-form programmable optical frequency filter," in *Proc. ECOC'94*, 1994, We. P. 19.
[10] K. Takiguchi, K. Jinguji, and Y. Ohmori, "Variable group-delay dispersion equalizer based on a lattice-form programmable optical filter," *Electron. Lett.*, vol. 31, no. 15, pp. 1240–1241, 1995.
[11] K. Takiguchi, K. Jinguji, K. Okamoto, and Y. Ohmori, "Variable group-delay dispersion equalizer using lattice-form programmable optical filter on planar lightwave circuit," *IEEE J. Select. Topics Quantum Electron.*, vol. 2, pp. 270–276, Feb. 1996.
[12] A. V. Oppenheim and R. W. Schafter, *Digital Signal Processing*. Englewood Cliffs, NJ: Prentice-Hall, 1975.
[13] K. Jinguji and M. Kawachi, "Synthesis of coherent two-port lattice-form optical delay-line circuit," *J. Lightwave Technol.*, vol. 13, pp. 73–82, Jan. 1995.
[14] K. Jinguji, "Synthesis of coherent two-port optical delay-line circuit with ring waveguides," *J. Lightwave Technol.*, vol. 14, pp. 1882–1898, Aug. 1996.
[15] C. K. Madsen, "Efficient architectures for exactly realizing optical filters with optimum bandpass designs," *IEEE Photon. Technol. Lett.*, vol. 10, pp. 1136–1138, Aug. 1998.
[16] P. P. Vaidyanathan, P. A. Regalia, and S. K. Mitra, "Design of doubly-complementary IIR digital filters using a single complex allpass filter, with multirate applications," *IEEE J. Trans. Circuits Syst.*, vol. CAS-34, pp. 378–389, Apr. 1987.
[17] S. K. Mitra and J. F. Kaiser, *Handbook for Digital Signal Processing*. New York: Wiley, 1993, ch. 7.
[18] H. Kumazawa and I. Ohtomo, "30 GHz-band periodic branching filter using a traveling-wave resonator for satellite applications," *Trans. Microwave Theory Tech.*, vol. MTT-25, pp. 683–687, 1977.
[19] R. Watanabe and N. Nakajima, "Reflection type periodic filter with two-resonators using Gaussian beam at millimeter-wave region," *Trans. IEICE*, vol. J 62-B, no. 11, pp. 990–997, 1979.
[20] K. Oda, N. Takato, H. Toba, and K. Nosu, "A wide-band guided-wave periodic multi/demultiplexer with a ring resonator for optical FDM transmission systems," *J. Lightwave Technol.*, vol. 6, pp. 1016–1023, June 1988.
[21] M. Kawachi, "Silica waveguides on silicon and their application to integrated-optic components," *Optic. Quantum Electron.*, vol. 22, pp. 391–416, 1990.
[22] K. Jinguji, N. Takato, Y. Hida, T. Kitoh, and M. Kawachi, "Two-port optical wavelength circuits composed of cascaded Mach–Zehnder interferometers with point-symmetrical configurations," *J. Lightwave Technol.*, vol. 14, pp. 2301–2310, Oct. 1996.
[23] C. Gumacos, "Weighting coefficients for certain maximally flat nonrecursive digital filters," *IEEE J. Trans. Circuits Syst.*, vol. CAS-25, pp. 234–235, Apr. 1978.
[24] J. H. McClellan, T. W. Parks, and L. R. Rabiner, "A computer program for designing optimum FIR linear phase digital filters," *IEEE Trans. Audio Electroacoust.*, vol. AU-21, pp. 506–526, June 1973.
[25] A. H. Gray and J. D. Markel, "Computer program for designing digital elliptic filters," *IEEE Trans. Acoust., Speech, Signal Processing*, vol. ASSP-24, pp. 529–538, June 1976.

Kaname Jinguji was born in Osaka, Japan, on December 12, 1952. He received the B.S. and M.S. degrees in applied physics, and the Ph.D. degree in electronic engineering from Osaka University, Osaka, Japan, in 1975, 1977, and 1998, respectively.

In 1977, he joined NTT Ibaraki Electrical Communications Laboratories, Ibaraki, Japan, where he was engaged in research on characteristics analysis of optical silica and plastic fibers. His current research interests are centered around computer analysis of transmission characteristics and circuit synthesis for optical waveguides and optical integrated circuits.

Dr. Jinguji is a member of the Institute of Electronics, Information and Communication Engineers (IEICE) of Japan.

Manabu Oguma was born in Hokkaido, Japan, on April 7, 1966. He received the B.S. and M.S. degrees in applied physics from Tohoku University, Sendai, Japan, in 1989 and 1991, respectively.

He joined the NTT Opto-Electronics Laboratories (now Photonics Laboratories), Ibaraki, Japan, in 1991, where he has been engaged in research on optical waveguide devices.

Mr. Oguma is a member of the Japan Society of Applied Physics.